International Journal of Hydrogen Energy 87 (2024) 1129–1139

Contents lists available at ScienceDirect

International Journal of Hydrogen Energy

journal homepage: www.elsevier.com/locate/he

Investigation of the performance and emission effects of ammonia-borane as a B–N-based amine-borane adduct in gasoline engines

Ahmet Yakin [a,*], Mehmet Gülcan [b], Samet Çelebi [c,d], Usame Demir [e], Emre Yilmaz [c]

[a] Department of Motor Vehicles and Transportation Technologies, Van Vocational School, Van Yüzüncü Yıl University, 65080, Van, Turkey
[b] Chemistry Department, Faculty of Science, Van Yüzüncü Yıl University, Zeve Campus, 65080, Van, Turkey
[c] Department of Motor Vehicles and Transportation Technologies, Arifiye Vocational School, Sakarya University of Applied Sciences, Sakarya, Turkey
[d] Sakarya University of Applied Sciences Automotive Technologies Application and Research Center, Turkey
[e] Bilecik Şeyh Edebali University, Engineering Faculty, Department of Mechanical Engineering, 11100, Bilecik, Turkey

ARTICLE INFO

Keywords:
Ammonia-borane
Engine performance
Exhaust emissions
Gasoline engine

ABSTRACT

This study examined the impact of varying concentrations of ammonia-borane (AB) in gasoline on engine performance and emissions across different load conditions. Four fuel formulations were tested: pure gasoline (G100) and gasoline blends containing 10%, 15%, and 20% AB (AB10, AB15, AB20). Increased AB concentration resulted in higher brake-specific fuel consumption (BSFC). While exhaust gas temperatures were highest with G100 (730.9 °C at full load), the AB blends, particularly AB20, exhibited lower temperatures, with a maximum reduction of 13.8%. The AB20 blend demonstrated elevated BSFC and increased oxygen (O_2) emissions but significantly reduced carbon monoxide (CO) emissions, with up to an 88.2% decrease at full load. Nitrogen oxide (NO_x) emissions were generally lower for all AB blends. The highest NO_x value was measured with G100 fuel at full load, while the lowest NO_x value was measured with AB10 fuel. Under these conditions, a 23% decrease in NO_x value was observed with AB10 fuel compared to G100. The engine's thermal efficiency decreased with AB blends at all load levels compared to pure gasoline. Thermal efficiency decrease of 13.76%, 22.32%, and 30.88% occurred for AB10, AB15 and AB20, respectively compared to G100.Overall, incorporating AB in gasoline reduced thermal efficiency and led to a notable decrease in NO_x, hydrocarbons (HC), and CO emissions.

1. Introduction

The rising global energy demand and environmental issues associated with fossil fuel use have spurred the pursuit of alternative and sustainable energy sources. This synthesis examines recent research on alternative energy, highlighting the challenges and potential solutions for decreasing dependence on fossil fuels [1]. Countries with abundant fossil fuel reserves have experienced a rise in fossil fuel demand but minimal expansion in renewable energy usage, which poses a considerable challenge to climate change mitigation efforts [2]. Immediate and transformative changes are necessary to limit global warming to below 2 °C [3]. The continued availability of fossil fuels drives their use, highlighting the need for strong policies and strategies to transition towards non-carbon-emitting technologies [4]. Rising fuel prices, energy demand, and global warming concerns drive interest in bioenergy [5,6]. Biofuels, particularly bioethanol, have become competitive with petroleum in many countries, offering a renewable alternative that can reduce carbon emissions [7] and promote agricultural sustainability [8,9]. Bioenergy is seen as a significant contributor to rural economic development and poverty reduction through job creation and improved quality of life [10]. Increasing energy demand and environmental concerns related to the use of fossil fuels have brought the search for alternative and sustainable fuels to the forefront [11]. Gasoline, the primary fuel used for spark ignition (SI) engines, is derived from petroleum and contributes significantly to greenhouse gas emissions and air pollution [12]. To overcome these challenges, researchers are investigating the potential of fuel additives to improve performance and reduce the environmental impact of gasoline-powered engines [13].

The use of alcohol additives in gasoline for spark ignition engines has been extensively studied due to their potential to reduce greenhouse gas emissions and improve fuel properties [14]. Alcohols such as ethanol, methanol, and higher alcohols like iso-butanol and iso-amyl alcohol are considered promising alternatives to traditional gasoline due to their favorable physicochemical properties and environmental benefits [15]. Alcohol-gasoline blends generally result in lower emissions of carbon

* Corresponding author.
E-mail address: ahmetyakin@yyu.edu.tr (A. Yakin).

https://doi.org/10.1016/j.ijhydene.2024.09.117
Received 12 June 2024; Received in revised form 6 September 2024; Accepted 10 September 2024
Available online 14 September 2024

Symbols and abbreviations

C_8H_{18}	Octane
C_2H_5OH	Ethanol
CH_3OH	Methanol
G100	Gasoline
AB10	%90 Gasoline + %10 Ammonia-borane
AB15	%85 Gasoline + %15 Ammonia-borane
AB20	%80 Gasoline + %20 Ammonia-borane
CO	Carbon monoxide
HC	Hydrocarbon
NO_x	Nitrous oxide
CO_2	Carbon dioxide
O_2	Oxygen
n	Engine speed
Me	Engine torque
Ne	Engine power
be	Brake specific fuel consumption
LHV	Lower calorific value
BSFC	Brake specific fuel consumption
EGT	Exhaust gas temperature

monoxide (CO), nitrogen oxides (NO_x), and hydrocarbons (HC) compared to pure gasoline [16,17].

Ethanol-gasoline blends have been shown to significantly decrease CO and HC emissions in various operating conditions [18]. Blending alcohols with gasoline can enhance engine performance metrics such as brake thermal efficiency (BTE) [19], brake power [20], and torque [21,22]. Higher alcohols like iso-butanol and isoamyl alcohol, when added to gasoline, improve engine performance and efficiency, particularly at higher compression ratios [23,24]. Alcohol additives improve the octane number of gasoline, leading to better anti-knock properties and more efficient combustion [25–28]. Dual-alcohol blends (e.g., methanol and iso-butanol) can achieve vapor pressures close to that of base gasoline, optimizing volatility and reducing evaporative emissions [29,30]. Alcohols contribute to more complete combustion due to their higher oxygen content, which enhances combustion efficiency and reduces soot formation [31,32]. The presence of oxygen in alcohol molecules and their faster flame speeds lead to improved combustion initiation and stability [33,34]. While alcohols improve many aspects of engine performance and emissions [35], they can also increase specific fuel consumption [36] due to their lower energy content [37] compared to gasoline.

Boron-based additives have been explored for their potential to enhance the performance and reduce emissions of internal combustion engines [38]. These additives, which include ammonia-borane (AB, NH_3BH_3) [39] and trimethyl-borate [40], are investigated for their effects on fuel efficiency, combustion characteristics, and emission profiles. AB increases the burn rate of ethanol by 16% due to gas formation and droplet shattering during combustion, leading to rapid combustion of the remaining fuel [41]. These boron-based additives, also known as amine-boranes, are promising fuel additives with a proven ability to improve engine performance and reduce emissions [42] and are known for their high energy density as well as their ability to suppress knocking, one of the factors that hinder engine efficiency [43,44].

Boron-based compounds, such as methylamine-borane [45] and dimethylamine-borane [46–48], especially AB, have become central to hydrogen energy research due to their high hydrogen densities in solid form. Researchers note that hydrogen (H_2), a clean and renewable fuel, will play a significant role in transitioning from traditional fossil fuels to renewable energy sources on the path to a sustainable energy future. However, the most significant challenges for H_2 are its safe storage and transportation. Among the boron-based compounds mentioned above, AB is known as the simplest boron-nitrogen adduct with a molecular weight of 30.87 g/mol and a hydrogen storage capacity of up to 19.6% by weight. AB, first successfully synthesized by Shore and Parry in 1955, is one of the most promising hydrogen carrier materials, being stable under ambient conditions, having a high gravimetric hydrogen content, being environmentally friendly, and highly soluble in most polar solvents like ethanol/methanol. AB can release the stored hydrogen in its solid form through dehydrogenation, hydrolysis, and methanolysis reactions with a suitable catalyst when needed [49–53].

This study aims to investigate the impact of incorporating various ratios of AB along with fuel additives into gasoline on the performance and emissions characteristics of gasoline engines. The primary focus is to evaluate how these additives influence key engine parameters such as power output, fuel efficiency, and the emissions of pollutants like carbon monoxide (CO), hydrocarbons (HC), and nitrogen oxides (NO_x). Through rigorous experimental analysis, we seek to assess the potential of AB additives as viable alternatives to traditional gasoline. Specifically, we determine the optimal ratios of these additives in gasoline formulations to achieve peak engine performance while minimizing harmful exhaust emissions. Furthermore, the study explores actionable strategies for enhancing engine efficiency and reducing emissions by applying AB additives. The study investigates how adding AB and fuel additives to gasoline affects engine performance and emissions. It emphasizes the goal of identifying optimal additive ratios to improve engine efficiency and reduce harmful pollutants, positioning AB as a potential alternative to conventional gasoline additives. The desired activities related to blended fuels are shown in Fig. 1 as a flow chart.

2. Experimental studies

2.1. Materials

In this study, the sodium borohydride ($NaBH_4$), ammonium sulfate ($(NH_4)_2SO_4$), tetrahydrofuran (C_4H_8O, THF) used to synthesize AB as a fuel additive, and the ethanol (C_2H_5OH) used to prepare gasoline-AB fuel mixtures were commercially obtained from Sigma-Aldrich.

2.2. Synthesis of AB

Previous studies were utilized to synthesize AB. For this purpose, $NaBH_4$ (1.0 mol) and powdered $(NH_4)_2SO_4$ (1.0 mol) were placed in a three-neck round-bottom flask equipped with a reflux condenser. One neck of the three-neck flask was connected to an oil trap via a connecting tube. Pre-dried THF was then added to the reaction flask, and the mixture was stirred at 750 rpm at 40 °C for approximately 2 h. The mixture was then cooled to room temperature, and the solid part was isolated by filtration. The filtrate was evaporated under vacuum to remove THF [54,55].

2.3. Characterization

X-ray diffraction (XRD, Rigaku Ultima-IV with Cu-Ka radiation, wavelength 1.54 Å, 40 kV, 55 mA) and Fourier transform infrared (FT-IR, Shimadzu IR-Affinity instrument using KBr disks in the 500-4000 cm^{-1} region) analyses were applied to determine the crystal properties and to identify the functional groups in the chemical structure of the synthesized AB, respectively. Elemental analysis (EA; C, H, N, S–O) was carried out with Thermo Scientific Flash 2000 analysis instrument. ^{1}H and ^{11}B-NMR were also used for the characterization of the structure of AB. The measurements were carried out with a Bruker 400 MHz Avance III Topspin 2.1 Spectrometry/Darmstadt/Germany. Samples were solved in DMSO-d_6 before the analysis, and all measurements were taken at room temperature.

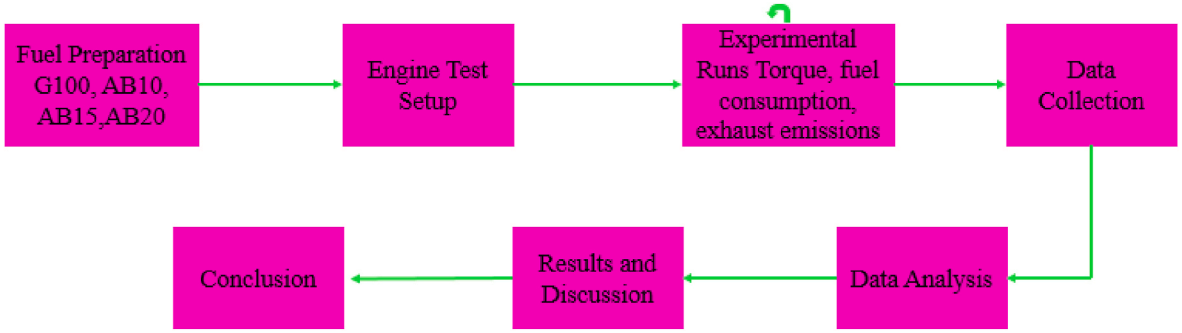

Fig. 1. Flow diagram of experiments.

2.4. Preparation of fuel mixture

Three different fuel types were created: AB10 blend fuel consisting of 10% AB and 90% gasoline by volume, AB15 blend fuel consisting of 15% AB and 85% gasoline, and AB20 blend fuel consisting of 20% AB and 80% gasoline, respectively. Thus, four test fuel types, one pure gasoline, were prepared for use in the experiments. The flow diagrams of the blended fuels are given in Fig. 2.

The experimental mixture fuels were analyzed at the Fuel Analysis Laboratory of the Department of Automotive Engineering, Adana Cukurova University. The physical and chemical properties of the blended fuels are given in Table 1.

The experimental fuels were analyzed at the Fuel Analysis Laboratory of the Department of Automotive Engineering, Adana Cukurova University.

2.5. Experimental setup

The blended fuels prepared at Van Yüzüncü Yil University, Faculty of Science, Department of Chemistry were tested in the engine test laboratories of Sakarya University of Applied Sciences, Arifiye Vocational School, Department of Motor Vehicles and Transportation Technologies. The experimental study was conducted on a single-cylinder air-cooled spark ignition Honda GX200 model engine. The technical specifications of the engine in which the blended fuels were tested are given in Table 2.

The schematic picture of the experimental setup is given in Fig. 3. In the setup, there's a fuel tank that would contain test fuel. The fuel tank is placed on a precision scale. This precision scale has an accuracy of 0.01 g. Fuel consumption values are calculated by dividing the amount of fuel consumed in 1 min by the engine power with this sensitive scale. A Plint&Partners electric dynamometer was used during the experiment to control the engine by braking precisely. The experimental engine was connected to the dynamometer via a coupling. By checking the

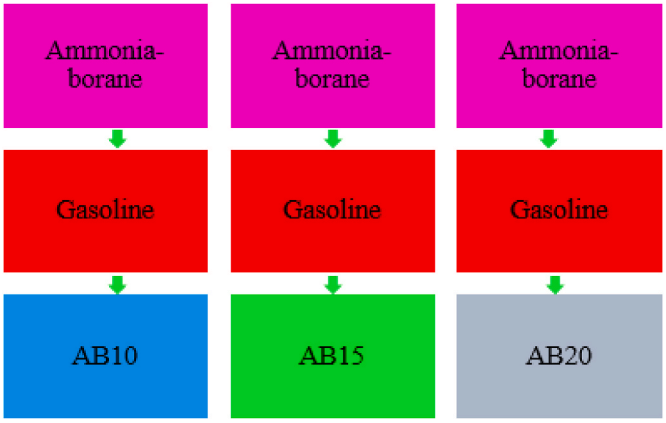

Fig. 2. Flow diagram of preparation of AB10, AB15, AB20 mixture fuels.

Table 1
Properties of the fuels used in the experiments.

Fuel specifications	G100	AB10	AB15	AB20
Kinematic viscosity (40 °C) mm^2/s	0.65–0.80	0.86	0.865	0.85
Density (g/cm^3)	720–750	752	754	756
Octane number	95	90.9	88.72	86.2
Lower heating value (cal/g)	10400	10115.7	9957.425	9746.2

Table 2
Test engine specifications.

Test Engine	Honda GX200
Compression ratio	8.5/1
Cooling System	Forced air
Cylinder number	1
Engine Type	4 Stroke, Over Head Valve
Maximum engine speed (rpm)	3600
Maximum torque (Nm/2500 rpm)	12.4
Maximum power (kW/3000 rpm)	4.8
Volume (cm^3)	196
Bore x stroke (mm)	68 x 54

dynamometer with the help of the control panel, the test engine was given the first movement (starter) with the dynamometer, the engine was loaded after the engine was started. When the electric dynamometer works as a starter, it provides the necessary direct current by converting the alternating current in the network into direct current by a rectifier. After the engine starts, the control key is turned to the dynamometer position to load the test engine. The installation process is achieved by switching on and off the resistor at the output of the dynamometer. A bar-type load cell with 0.1 kg sensitivity was connected to the dynamometer to measure the power produced by the test engine. The load cell was calibrated precisely before the experiments. As the engine runs, it creates exhaust gases that flow through a pipe. The temperature of exhaust gases is measured because it tells us how well the fuel is burning. Too hot might mean the engine is running too lean, and too cool might suggest incomplete combustion. For exhaust gas temperature measurement, exhaust gas temperature was measured with a K-type thermocouple placed in the exhaust manifold.

2.6. Test procedure

The tests were carried out at a constant 2500 rpm, where the engine's maximum torque value is. The engine was loaded under five different loads at this speed, and experiments were carried out. Engine tests were measured for full loading (100%), 75%, 50%, 25% loadings and no load situations. Each experiment was repeated three times, and the arithmetic average of the results was recorded.

There is an emissions measuring device, which is an essential part of this setup. It analyzes the exhaust gases to determine the levels of

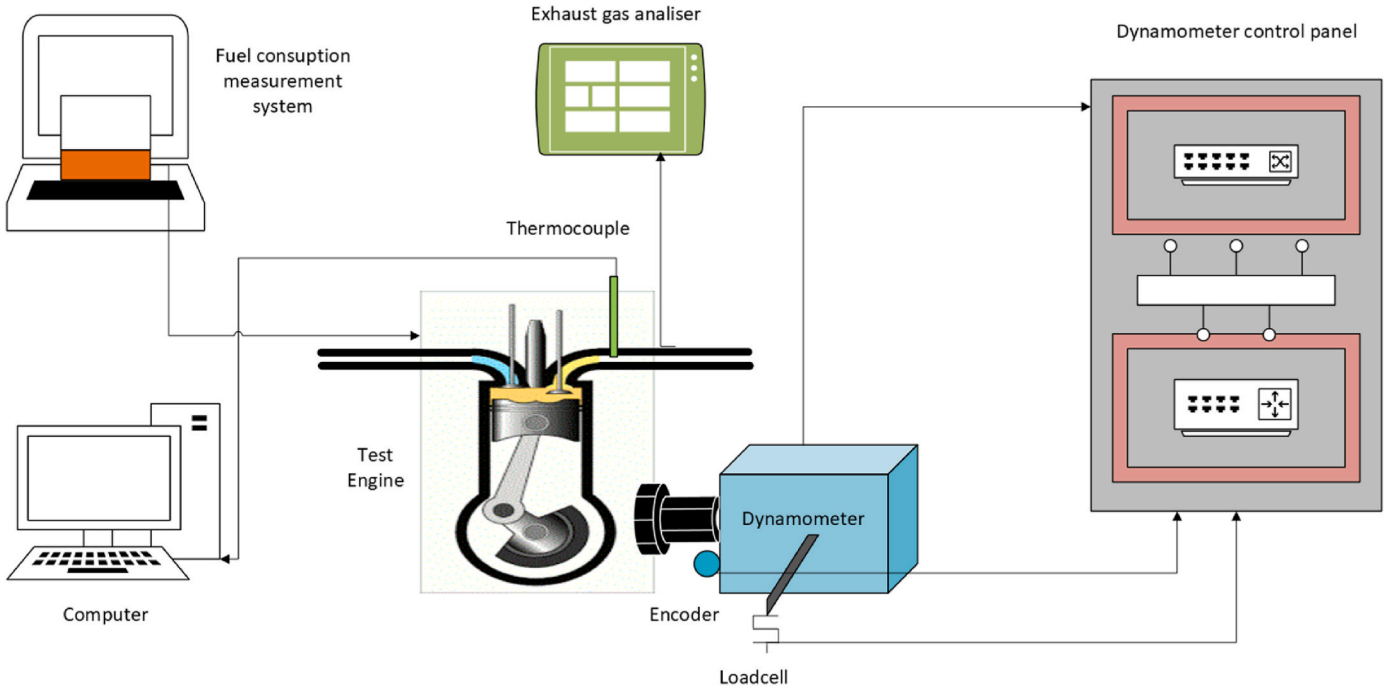

Fig. 3. The schematic view of the experimental setup.

various pollutants the engine emits, such as carbon monoxide, nitrogen oxides, and unburned hydrocarbons. These measurements help us understand the environmental impact of the fuel being tested and are crucial for making sure that the fuel meets regulatory standards. The exhaust emissions measurements were done by connecting the device's exhaust emissions measurement apparatus to the experimental engine's exhaust outlet pipe. Technical specifications of the exhaust emission device (Bosch BEA 460 brand emission device) used in the experiments are given in Table 3.

2.7. Uncertainty analysis

In the measurement of a parameter, the total error is calculated using Equation (1), which considers manufacturing errors, fixed errors, and random errors. The uncertainty in W_R, derived from a function R of independent variables x_1, x_2, …, x_n, is determined by the uncertainties w_1, w_2, …, w_n associated with these variables [56].

$$W_R = \left[\left(\frac{\partial R}{\partial X_1} W_1 \right)^2 + \left(\frac{\partial R}{\partial X_2} W_2 \right)^2 + \ldots + \left(\frac{\partial R}{\partial X_n} W_n \right)^2 \right]^{\frac{1}{2}} \quad (1)$$

Table 3 provides uncertainties for engine speed and emissions (CO, CO_2, HC, O_2). Manufacturer specifications indicate uncertainties of ±1 °C for air temperature, ±0.5% for CO, ±2% for CO_2, ±12% for HC, and ±0.4% for O_2. Also, ±0.02% for load cell, ±1% for engine speed, and ±0.1% for fuel consumption is calculated as.

Table 3
Technical specifications of the exhaust gas analyzer (Bosch BEA 460).

Component	Sensitivity	Tolerance
CO	0.001 %vol	±0.005 %vol
CO_2	0.01 %vol	±0.2 %vol
HC [ppm vol]	1	±12 ppm
O_2	0.01 %vol	±0.4 %vol
Lambda	0.001	–
NO [ppm vol]	1	–

3. Results and discussions

Before proceeding to motor performance and emission tests, melting point determination, FT-IR spectroscopy, XRD, EA, ^{1}H, and ^{11}B-NMR techniques were utilized to characterize the AB compound used as a fuel additive. The melting point of AB was determined to be 103 °C. This melting point was observed to be relatively consistent with the literature data [57]. The FT-IR spectrum provided for the AB compound (Fig. 4), along with its characteristic vibration regions, showed that the N–H stretching, B–H stretching, N–H deformation, B–H deformation, B–N stretching, and B–H stretching vibration peaks were highly consistent with the literature data [50]. This was considered evidence that the synthesis of AB was successfully carried out on a laboratory scale.

Based on previous studies, it is understood that synthetic AB has a crystalline structure. Therefore, an XRD analysis was performed to determine both the crystallinity and the characteristic diffraction

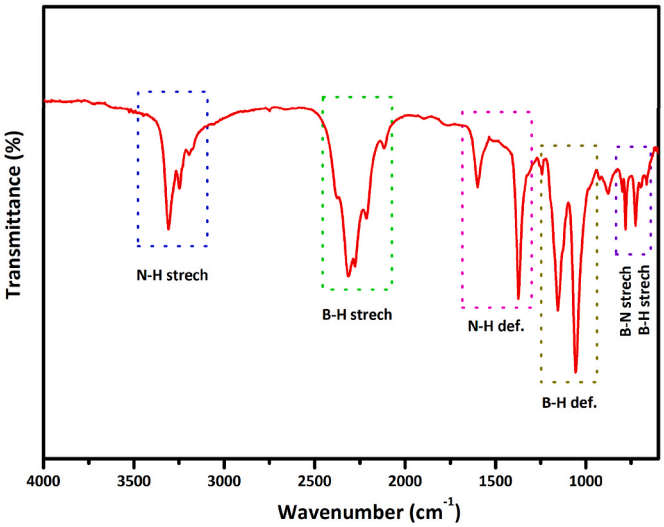

Fig. 4. FT-IR spectrum of AB.

reflections of the synthesized AB. Fig. 5 shows the XRD pattern of AB. AB has a tetragonal crystal structure. The characteristic reflection peaks at $2\theta = 24.2°$, 24.5°, 34.2°, 35.7°, 42.5°, 43.6°, 55.5°, and 57.7° prove that the product is highly crystalline when compared to the reference (01-074-0894 JPDS file) [58,59].

The elemental analysis results of the synthesized AB show 42.15% N and 18.08% H. When compared to 100% pure AB (45.38% N and 19.60% H), it was observed that the synthetic AB contained less than 1% (0.69%) C. According to the results, the product obtained with approximately 92% purity was found to be consistent with the reported literature results [54,55]. Furthermore, it was observed that the solvent used during the synthesis could be easily recycled using simple rotary evaporation and reused without any pre-purification.

Another piece of evidence that AB was synthesized with high purity can be observed in the ^{1}H and ^{11}B-NMR spectra. The ^{1}H and ^{11}B-NMR spectra of the samples prepared in DMSO-d_6 solvent are presented in Fig. S1 and Fig. S2, respectively. According to the NMR results, the observed chemical shift values were found to be quite similar to the literature values, indicating that the synthesis process was largely successful [54,55,60,61]. It should be noted that the signals observed at ~2.5 ppm and ~3.5 ppm in the ^{1}H NMR spectrum correspond to the chemical shift values of DMSO. Furthermore, the presence of partial impurity signals in the relevant spectrum, consistent with the elemental analysis results, indicates that a 100% pure product was not obtained.

Fig. 6 shows the variation of break-specific fuel consumption (BSFC) depending on the engine load. The BSFC values for each fuel type—G100, AB10, AB15, and AB20—decrease as the engine load increases from 25% to 100%. At 25% load, G100 has the lowest BSFC value of 776.69 g/kWh, while AB20 has the highest at 1216.56 g/kWh. At 50% load, the BSFC values are reduced for all fuels, with G100 again showing the lowest value of 541.20 g/kWh and AB20 the highest at 758.15 g/kWh. At 75% load, the trend continues similarly, with G100 at 418.64 g/kWh and AB20 at 664.11 g/kWh. At full load (100%), G100 has the most significant decrease in BSFC to 347.03 g/kWh, and AB20 shows the least efficiency with a value of 555.39 g/kWh. According to the graph, as the engine load increases, the specific fuel consumption decreases for all fuels. When the engine loads were 50%, 75%, and 100%, there was a 56%, 20%, 15% decrease in all fuels, respectively, compared to the 25% load case. The provided data clearly show that G100 consistently offers the best fuel efficiency across all engine loads, indicating that pure gasoline may provide more energy per unit of fuel consumed or that the engine is better optimized for this fuel type than the blends. The gradual decrease in BSFC values with increased engine loads is a common trend, as engines generally operate more efficiently at

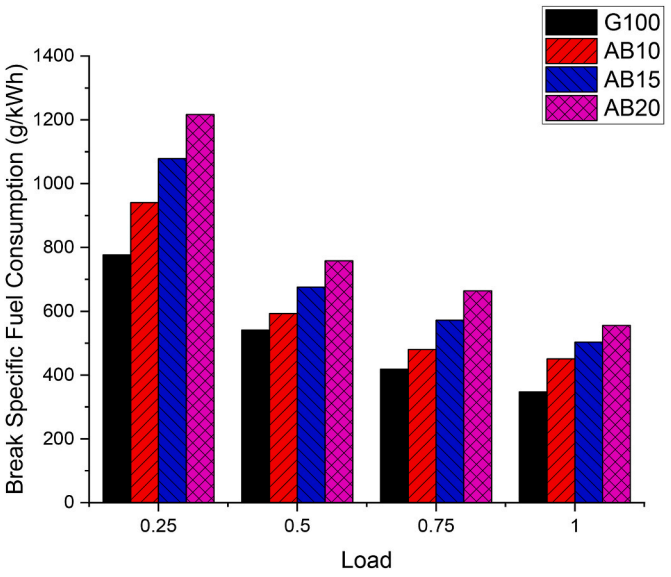

Fig. 6. Variation of break-specific fuel consumption with engine load.

higher loads. This is due to various factors, including better thermal efficiency and reduced relative friction losses at higher operating temperatures and pressures. AB10, AB15, and AB20 blends exhibit higher BSFC values at all loads than G100. AB20 has the highest values. When the fuel properties are examined, there has been an increase in the specific fuel consumption due to the decrease in the lower calorific value of the fuel, especially with the addition of AB fuel. It can be said that this especially depends on the lower calorific value of the fuel [17,25,36,62–64].

The variation of exhaust gas temperature depending on engine load is given in Fig. 7. The experimental measurements for exhaust gas temperatures were conducted at varying load percentages ranging from 0% to 100%. Four fuel types were analyzed: G100, AB10, AB15, and AB20. The results indicate that the exhaust gas temperatures varied with load and fuel type. The G100 fuel type exhibited the highest temperatures across all load levels, starting at 625.5 °C at 0% load and increasing to 730.9 °C at 100% load. This suggests a high level of combustion efficiency or possibly a higher energy content per unit volume. Compared to the G100, the AB10, AB15, and AB20 variants showed a decrease in exhaust temperatures at all load levels. The reason for this is the decrease in lower heating value due to adding the AB fuel additive. At

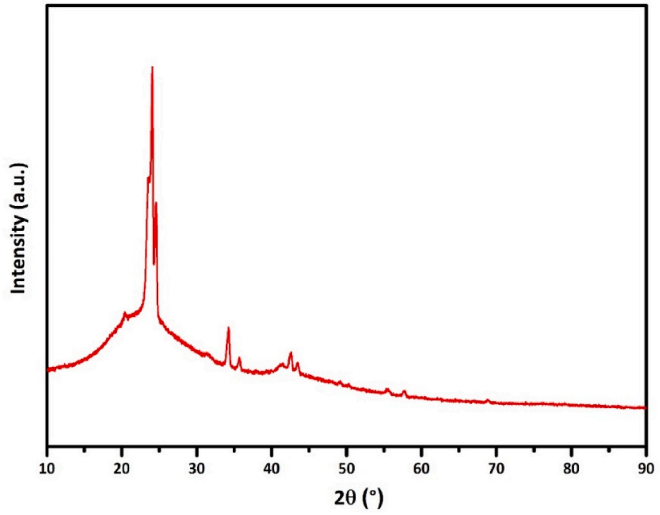

Fig. 5. XRD pattern of AB.

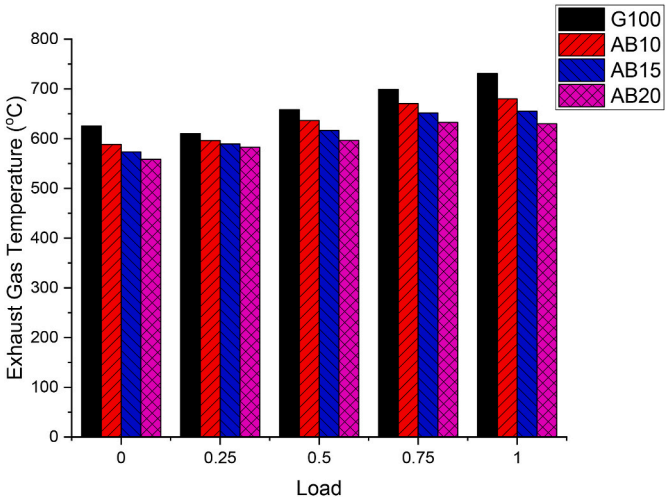

Fig. 7. Variation of exhaust gas temperature with engine load.

0% load, AB10 began at 588.2 °C, AB15 at 573.4 °C, and AB20 at 558.6 °C. These temperatures increased with the load, with AB10 reaching 680.1 °C, AB15 reaching 655.2 °C, and AB20 reaching 630.2 °C at 100% load, respectively. The blended fuels used in the engine, AB10, AB15, AB20, decreased by 4.58%, 7.16%, and 9.73%, respectively, compared to G100 fuel. The trend in the data indicates that the G100 fuel type, potentially pure gasoline, has a consistent increase in temperature with the load, which could be attributed to higher energy content and a consequent increase in the combustion temperature. In contrast, the blended fuels (AB10, AB15, and AB20) show a moderated temperature profile. At higher loads (50% and above), the difference in exhaust gas temperatures between G100 and the blends becomes more pronounced. This leads to a decrease in exhaust gas temperature. Additionally, the lower energy content and possible inefficiencies in the combustion process result in reduced power and torque outputs [65,66]. In the literature, studies with different fuel additives, such as phthalocyanine, have shown a decrease in exhaust gas temperature compared to gasoline fuel [67,68].

Fig. 8 shows the plot of O_2 emission variation with engine load. According to the graph, O_2 increased at all engine loads compared to gasoline fuel. The O_2 emission percentages show varying behavior across different loads for each fuel type. G100 starts at 1.7% O_2 emissions at 0% load and decreases to 0.9% at full load (100%). AB10 has initial O_2 emissions at 0.85%, almost half of G100's emissions at 0% load, but increases to 1.21% at full load. AB15 begins at 1.8% and shows a consistent increase across all loads, reaching 2.895% at full load. AB20 starts at 2.75% at no load and also increases to 4.58% at full load, showing the highest emissions among the fuels at most load levels. Each fuel shows a unique trend in O_2 emissions as engine load changes, with G100 decreasing while the others increasing with engine load, especially AB15 and AB20. According to the graph, the highest O_2 emission compared to gasoline fuel was 4.580% at 100% engine load with AB20 blend fuel.

The increased release of oxygen in the exhaust emissions with amine-borane additive fuels is primarily due to AB's hydrogen and nitrogen content. These elements alter the combustion chemistry, resulting in incomplete combustion and higher levels of unreacted oxygen in the exhaust gases. This phenomenon is more pronounced with higher AB concentrations, as evidenced by the higher O_2 emissions in AB20 compared to AB10 and AB15. Optimizing the combustion process and adjusting the air-fuel mixture for AB blends might help reduce these oxygen emissions. However, the current data indicates that the unique composition of AB significantly contributes to the observed increase in exhaust oxygen levels. This understanding is crucial for developing strategies to improve AB-gasoline blends' combustion efficiency and emissions profile, balancing performance benefits with environmental impacts [69–72].

CO emission is caused by incomplete combustion or incomplete combustion in internal combustion gasoline or diesel engines. The variation of engine load with CO emission is shown in Fig. 9. The maximum reduction of 78.34% occurred with AB20 fuel compared to gasoline fuel under 100% engine load. The experimental results show that the CO emissions vary with the type of fuel used as well as the engine load. For G100, the emissions start at 7.920 units (the units are not specified, likely parts per million or a percentage) at 0% load and decrease to 2.581 units at 100% load. This descending trend suggests that CO emissions from G100 fuel are higher at lower engine loads and decrease as the load increases. Compared to G100, the blended fuels (AB10, AB15, and AB20) display significantly lower CO emissions across all loads. AB10 emissions range from 3.700 units at 0% load to 1.725 units at 100% load. AB15 and AB20 both show an even greater reduction in emissions, with AB15 starting at 3.004 units at 0% load and falling to 1.014 units at 100% load and AB20 starting at 2.309 units at 0% load and sharply decreasing to 0.303 units at 100% load.

The observed reduction in CO emissions for the blended fuels compared to G100 could be due to the combustion characteristics of the blends, which may burn more completely or at different temperatures compared to pure gasoline (G100). The data suggest that blending gasoline with other substances (possibly lower carbon fuels or additives that enhance combustion efficiency) significantly reduces CO emissions, which is a desired outcome from an environmental standpoint since CO is a harmful pollutant [66]. The substantial decrease in CO emissions with increased engine load for all fuels could be due to higher temperatures and pressures at higher loads, which improve combustion efficiency and result in a more complete oxidation of carbon monoxide to carbon dioxide [73]. It is also interesting to note that the reduction in CO emissions is not linear with the increase in engine load, showing a more pronounced decrease between 0% and 50% load, after which the rate of decrease slows down. Among the blends, AB20 shows the lowest CO emissions at all engine loads, indicating that the blending ratio or the type of additive used in AB20 is most effective in reducing CO emissions. This might be due to a more optimized combustion process or the influence of additives that promote complete fuel burning. It is noteworthy that at 100% load, AB10 shows a slight increase in CO emissions

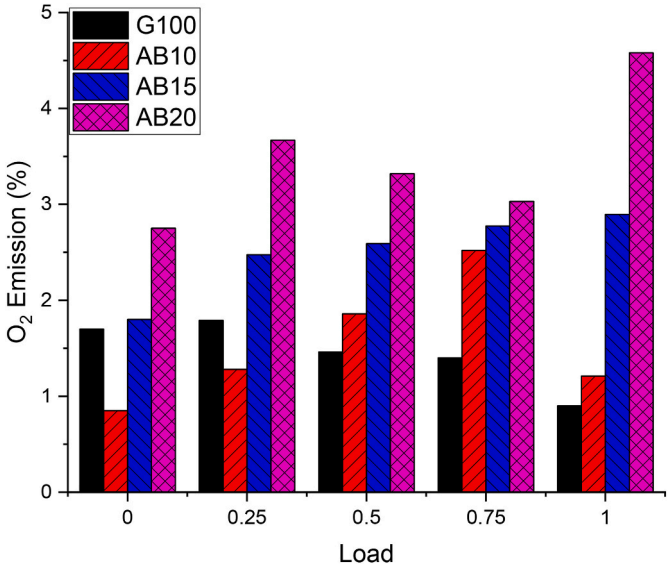

Fig. 8. Variation of O_2 with engine load.

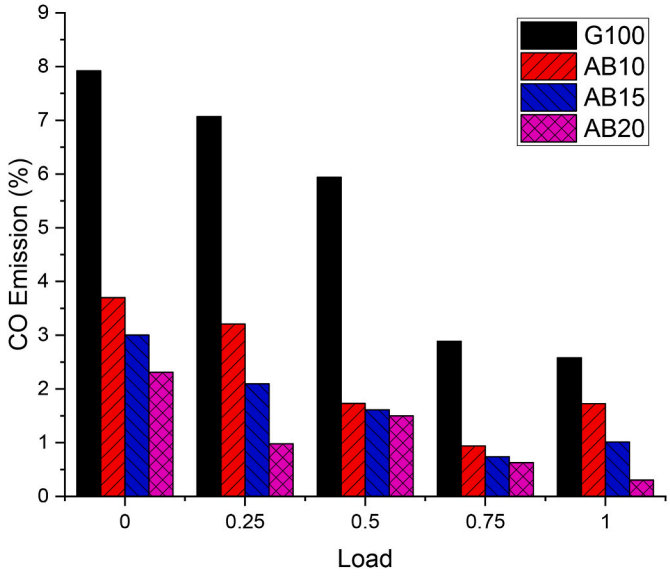

Fig. 9. Variation of CO emission with engine load.

compared to 75% load, which could be an anomaly or indicative of a characteristic of the blend that becomes apparent at full load. The study's findings have important implications for environmental sustainability and engine design. They suggest that using blended fuels can significantly lower CO emissions, which could contribute to meeting emission standards and improving air quality. Future research should delve into the specific compositions of the blends and their combustion properties to further understand the mechanisms behind the observed differences in CO emissions [74–78].

Fig. 10 shows the change graph of CO_2 emission depending on the engine load. CO_2 emission is an emission resulting from complete combustion. CO_2 emission is the amount of CO_2 released into the atmosphere. CO_2 is one of the greenhouse gases and causes climate change by increasing the temperature in the atmosphere. G100 shows a starting CO_2 emission of 8.250 at 0% load, increasing to 12.900 at full load. AB10 starts higher than G100 at 0% load with 12.950 and rises to 13.560 at full load, showing the highest emissions at all load levels. AB15 begins at 12.735 at no load and goes up to 12.720 at full load. AB20 starts at 12.520 at 0% load, which is higher than G100 but lower than AB10 and AB15. It increases to 11.880 at 100% load, which is notably lower than all other fuels at full load. Across all fuels, the percentage of CO_2 emissions increases as the load increases, which is typical as more fuel is consumed to produce more power. When the graph is analyzed, CO_2 emission of blended fuels increased compared to gasoline fuel at all engine loads. The highest rate of increase in CO_2 emissions compared to gasoline fuel was 22.31% with AB10 blend fuel.

The progression of CO_2 emissions with increasing engine load is consistent with expected combustion behavior, where higher loads demand more fuel, resulting in greater CO_2 emissions. The G100 fuel, likely pure gasoline, exhibits the lowest initial CO_2 emissions but steadily rises as the load increases. This could suggest that G100 is more efficient at lower loads but reaches similar efficiency levels as the blends at full load. The blends (AB10, AB15, and AB20) have higher initial CO_2 emissions at no load compared to G100, which may be attributed to less optimal combustion when the engine is not under significant load. The high starting point for AB10 could imply that this blend is less efficient than G100 at low load levels.AB20 presents an interesting case; despite starting with higher emissions at no load compared to G100, it ends with the lowest emissions at full load among all fuel types. This might indicate that the composition of AB20 offers better combustion efficiency or a higher oxygen content at higher operational loads, leading to more complete fuel burning and reduced CO_2 production. The fact that AB15 and AB20 show a decrease or a smaller increase in emissions from 75% to 100% load compared to the other fuels might suggest that these blends maintain better efficiency or combustion stability at high loads. This characteristic could be particularly advantageous in real-world settings where engines often operate at high loads. It is important to note that while CO_2 is not a pollutant in the traditional sense, it is a significant greenhouse gas, and its reduction is vital for addressing climate change. The use of gasoline and its blends can be part of a strategy to mitigate environmental impact since these fuels are derived from renewable sources and may have a lower carbon footprint over their lifecycle compared to fossil fuels [75]. Studies in the literature have shown that the addition of various fuel additives such as phthalocyanine to blended fuels results in decreased CO emissions compared to pure gasoline [67,68,79].

The HC emission change graph of the experimental fuels depending on the engine load is given in Fig. 11. The results indicate a clear trend of decreasing emissions with increasing engine load for all fuel types. G100 displayed the highest HC emissions at no load with 248 ppm, significantly dropping to 38 ppm at full load. AB10 started with considerably lower emissions than G100 at 0% load (49 ppm) and saw a reduction to 34 ppm at full load. AB15 had an initial emission value of 64.5 ppm at 0% load, which is notably lower than the other fuels, and decreased to 35 ppm at 100% load. AB20 started with 80 ppm at no load and also showed a decrease, reaching 35.5 ppm at full load. The data illustrate a consistent reduction in HC emissions as the engine load increases for all fuel types, which is a common phenomenon as the higher temperatures and pressures at higher loads lead to more complete combustion. The maximum decrease was 42.84% at 100% engine load.

HC emission is the amount of hydrocarbons (HC) released into the atmosphere. HC emissions are gases that are formed during the complete combustion of fuel and vary depending on the structure of the fuel. HC emissions can form a flammable and explosive mixture in the air. They can also cause acid rain and damage the ozone layer. The marked decline in HC emissions with increased load for all fuels is typical due to the improved combustion efficiency at higher operational loads. The high initial HC emissions for G100 at idle could suggest poor combustion efficiency at low loads or that the fuel has a tendency to produce more unburnt hydrocarbons when the engine isn't under significant load. The blended fuels AB10, AB15, and AB20 begin with lower HC emissions at 0% load compared to G100, indicating better combustion efficiency at idle or possibly the presence of additives that reduce incomplete combustion. The lower initial emissions for AB15 and AB20 suggest these blends effectively reduce HC emissions even at low loads. AB10, while starting better than G100, shows a less consistent reduction pattern and increases HC emissions at full load compared to AB15 and AB20. This could imply that the blend components in AB10 are not as effective at maintaining low HC emissions under high load conditions as the other

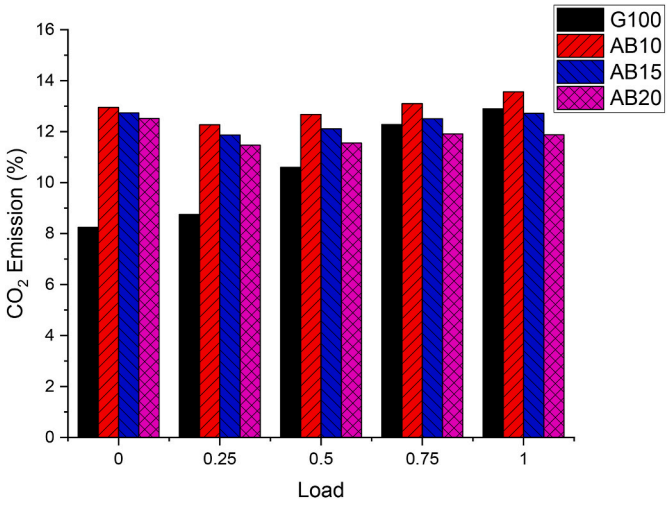

Fig. 10. Variation of CO_2 emission with engine load.

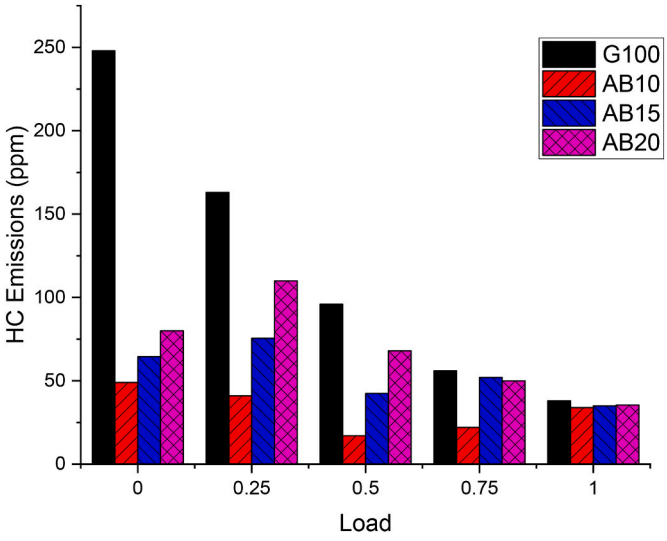

Fig. 11. Variation of HC emission with engine load.

blends. AB15 and AB20 stand out for their low emissions at high loads, suggesting that these fuel compositions may include components that promote better combustion or have inherent properties that result in fewer unburnt hydrocarbons. Certain additives in the blends could also be responsible for the catalytic conversion of HC emissions, even at lower temperatures. The difference between AB10's higher emissions at 100% load compared to AB15 and AB20 could be attributed to various factors, including the blend's specific components, their interaction with the engine's combustion chamber, and how they influence the combustion process at different loads. It's worth noting that HC emissions are a critical environmental concern since they contribute to smog formation and have health implications. Reducing HC emissions is an important objective for engine operation and fuel formulation. Future research should focus on the qualitative analysis of these emissions to understand the types of hydrocarbons emitted and how they may vary between the different fuel types and loads. Additionally, investigating the combustion characteristics of the fuels, the engine's efficiency with each type of fuel, and the role of potential additives could provide valuable insights into how to further reduce HC emissions. In conclusion, the data show that fuel composition and engine load significantly affect HC emissions. Blended fuels, especially AB15 and AB20, have demonstrated the potential to reduce HC emissions more effectively than pure gasoline (G100), especially at higher loads. This information could be vital for engine manufacturers and users when choosing fuels for both environmental considerations and engine performance [80–83].

Fig. 12 shows the variation of NO_x depending on the engine load. The experiment measured NO_x emissions for four fuel types at various engine loads, from idle (0%) to full load (100%). G100 showed increasing NO_x emissions from 15 ppm at 0% load to 65 ppm at 100% load. AB10 started with much lower emissions at 7 ppm at 0% load, increasing to 50 ppm at 100% load. AB15 had the lowest initial emissions at 8.5 ppm at 0% load, with a slight increase to 55 ppm at full load. AB20 emissions began at 10 ppm at 0% load and rose to 60 ppm at 100% load. For all fuels, NO_x emissions increase as the engine load increases, which aligns with typical combustion engine behavior where higher combustion temperatures at increased loads facilitate NO_x formation.

The data suggest a clear trend of increasing NO_x emissions with engine load for all tested fuel types. NO_x emissions are predominantly formed in high-temperature environments, explaining the higher emissions observed at elevated engine loads.G100 shows a consistent and significant increase in NO_x emissions with engine load. Being possibly pure gasoline, G100 may combust at higher temperatures, promoting NO_x formation, especially under high-load conditions [76,84–86].

Fig. 13 presents the thermal efficiency of various gasoline-AB blends—G100 (pure gasoline), AB10, AB15, and AB20—across different engine loads (0.25, 0.5, 0.75, and 1). The thermal efficiencies are expressed as percentages. At a load of 0.25, G100 exhibits an efficiency of 10.64%. Among the AB blends, AB10 shows the highest efficiency at this load with 12.09%, followed by AB15 at 11.01%, and AB20 at 9.91%. As the load increases to 0.5, the efficiency of G100 rises to 15.27%. The AB blends display improved efficiencies compared to G100, with AB10 achieving 14.33%, AB15 reaching 12.98%, and AB20 at 11.63%. At a load of 0.75, G100's efficiency increases to 19.75%, while the AB blends continue to follow a similar trend: AB10 records 17.70%, AB15 at 15.48%, and AB20 at 13.27%. At full load (1), G100 attains its highest efficiency at 23.82%. Among the AB blends, AB10 demonstrates the highest efficiency at 18.85%, followed by AB15 at 17.36%, while AB20, which had shown higher efficiency than G100 at lower loads, achieves 15.87%, falling behind the other blends at full load.

The results indicate a decline in thermal efficiency across all engine loads with the incorporation of ammonia-borane (AB) into gasoline. Pure gasoline (G100) demonstrates a steady increase in efficiency as the engine load increases, reaching a maximum efficiency of 23.82% at full load. In contrast, adding AB (AB10, AB15, AB20) leads to a marked reduction in thermal efficiency, particularly at higher loads. Among the AB blends, AB10 consistently exhibits the highest efficiency at all load levels. At a load of 0.25, AB10 achieves an efficiency of 9.03%, which is lower than G100 but higher than both AB15 and AB20. As the load increases, AB10 records efficiencies of 14.33% at 0.5 load and 17.70% at 0.75 load. AB10 achieves the highest efficiency at full load among the AB blends, with a value of 18.85%. AB15 also shows improvements relative to G100, particularly at higher loads, achieving 12.98% efficiency at 0.5 load, 15.48% at 0.75 load, and 17.36% at full load, though it remains lower than G100 and AB10. AB20 exhibits lower efficiencies than G100 at low and high loads, recording 11.63% at 0.5 load, 13.27% at 0.75 load, and 15.87% at full load. AB10 consistently shows higher efficiency at elevated loads than AB15 and AB20 [38,41].

Nie et al. (2024) conducted a study that assessed the impact of ammonia-diesel dual fuel combustion at various altitudes on several parameters, including in-cylinder pressure, heat release rate, in-cylinder temperature, ignition delay, CA50, combustion duration, and emissions like NO_x, ammonia (NH_3), and CO_2. The results indicated that as the rate of ammonia substitution increased, there was a significant reduction in NO_x and CO_2 emissions. However, the levels of unburned NH_3, particle

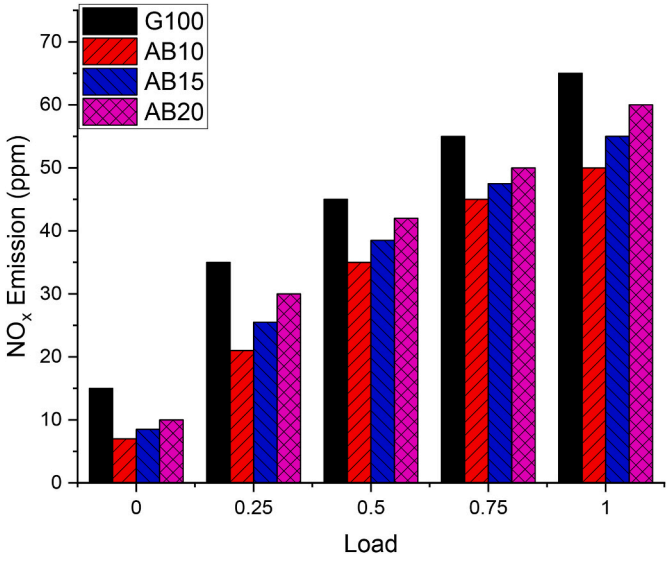

Fig. 12. Variation of NO_x emission with engine load.

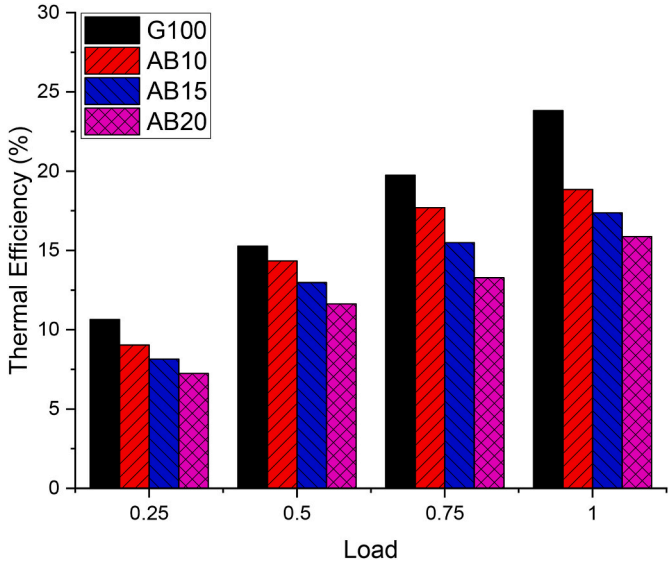

Fig. 13. Variation of thermal efficiency with engine load.

number (PN), total hydrocarbons (THC), and CO emissions rose [87]. Liu et al. (2024) aimed to investigate the combustion and emission performance of a single-cylinder spark ignition engine fueled with ammonia and gasoline mixtures under various operating conditions. The study examined the effects of ammonia (NH_3) mixture ratio, engine load, EGR rate, engine speed, intake variable valve timing (VVT) phase, fuel composition, and octane rating. The findings indicated that NH_3 mixtures can effectively reduce knock, optimize combustion timing, improve thermal efficiency, and lower NO_x emissions [88]. In addition to these benefits, achieving higher energy efficiency is also supported by advancements such as new geometric designs in heat sinks and the application of nanofluids [89,90].

4. Conclusion

In this study, the performance and exhaust emissions of AB10, AB15, and AB20 blend fuels were experimentally investigated as fuel in a four-stroke, single-cylinder gasoline engine, and the results obtained are listed below:

- According to the test results made with the AB20 mixture compared to G100 under full load conditions, it is seen that the BSFC value increases by 60.04%. When compared to pure gasoline, it is seen that the BSFC value increases as the AB amount in the mixture content increases. This situation shows that the energy required to meet the same engine torque increases due to lower heating values in the test points made under the same load conditions. When the data in the thermal efficiency graph is examined, the decreasing thermal efficiency values support this situation as the AB ratio in the mixture content increases.
- According to the test results conducted with the AB20 mixture compared to G100 under full load conditions, the thermal efficiency value decreases by 33.36%. Compared to pure gasoline, the thermal efficiency value decreases as the AB amount in the mixture content increases.
- The study suggests potential environmental benefits of AB blends, showing reductions in emissions such as CO, HC, and NO_x, indicating a favorable trade-off between performance degradation and environmental impact.

These findings underscore further research's need to optimize AB concentrations in fuel blends, aiming to balance performance gains with reductions in power output and fuel efficiency. Understanding AB's specific chemical and physical interactions in combustion processes could lead to tailored fuel formulations that optimize engine performance and environmental outcomes.

Future research

Future research could focus on several avenues to advance the study of amine-borane additives in gasoline engines. Investigating the synergistic effects of combining amine-borane with other fuel additives, such as antioxidants or combustion catalysts, could uncover optimized formulations that maximize engine performance and minimize emissions. Additionally, exploring the scalability and cost-effectiveness of producing amine-borane additives on a commercial scale would be crucial for their widespread adoption in the automotive industry. Further studies could also delve into the impact of these additives on exhaust after-treatment systems and their potential to facilitate compliance with stringent emissions regulations.

CRediT authorship contribution statement

Ahmet Yakin: Writing – original draft, Software, Resources. **Mehmet Gülcan:** Writing – review & editing, Software, Methodology, Formal analysis, Data curation. **Samet Çelebi:** Writing – review & editing, Software, Resources, Methodology, Data curation. **Usame Demir:** Writing – review & editing, Software, Resources, Methodology, Data curation, Conceptualization. **Emre Yilmaz:** Writing – review & editing, Writing – original draft, Software, Resources, Formal analysis.

Declaration of competing interest

The authors declare that they have no known competing financial interests or personal relationships that could have appeared to influence the work reported in this paper.

The authors declare the following financial interests/personal relationships which may be considered as potential competing interests:"Investigation of the performance and emission effects of ammonia-borane as a B–N-based amine-borane adduct in gasoline engines"

Acknowledgment

This study was supported within the scope of the Van Yüzüncü Yıl University Scientific Research and Application Center project numbered FYD-2022-10343.

Appendix A. Supplementary data

Supplementary data to this article can be found online at https://doi.org/10.1016/j.ijhydene.2024.09.117.

References

[1] Safaei R, Maihami R, Doranehgard MH, Silakhori M, Nikolaidis P, Poullikkas A. A Thorough emission-cost analysis of the gradual replacement of carbon-rich fuels with carbon-free energy carriers in modern power plants: the case of Cyprus. Sustain Times 2022;14:10800. https://doi.org/10.3390/SU141710800. 2022;14:10800.
[2] Johnsson F, Kjärstad J, Rootzén J. The threat to climate change mitigation posed by the abundance of fossil fuels. Clim Pol 2019;19:258–74. https://doi.org/10.1080/14693062.2018.1483885.
[3] Peters GP, Andrew RM, Boden T, Canadell JG, Ciais P, Le Quéré C, et al. The challenge to keep global warming below 2 °C. Nat Clim Chang 2012 2012;31(3):4–6. https://doi.org/10.1038/nclimate1783.
[4] Muradov NZ, Veziroğlu TN. "Green" path from fossil-based to hydrogen economy: an overview of carbon-neutral technologies. Int J Hydrogen Energy 2008;33:6804–39. https://doi.org/10.1016/J.IJHYDENE.2008.08.054.
[5] Banerjee S, Kaushik S, Tomar RS. Global scenario of biofuel production: past. present and future 2019:499–518. https://doi.org/10.1007/978-3-030-14463-0_18.
[6] McCarl BA, Maung T, Szulczyk KR. Could bioenergy Be used to harvest the greenhouse: an economic investigation of bioenergy and climate change? Handb Bioenergy Econ Policy 2010:195–218. https://doi.org/10.1007/978-1-4419-0369-3_12.
[7] Callegari A, Bolognesi S, Cecconet D, Capodaglio AG. Production technologies, current role, and future prospects of biofuels feedstocks: a state-of-the-art review. Crit Rev Environ Sci Technol 2020;50:384–436. https://doi.org/10.1080/10643389.2019.1629801.
[8] Saini JK, Saini R, Tewari L. Lignocellulosic agriculture wastes as biomass feedstocks for second-generation bioethanol production: concepts and recent developments. 3 Biotech 2015;5:337–53. https://doi.org/10.1007/S13205-014-0246-5/TABLES/8.
[9] Tse TJ, Wiens DJ, Reaney MJT. Production of bioethanol—a review of factors affecting ethanol yield. Ferment 2021;7:268. https://doi.org/10.3390/FERMENTATION7040268. 2021;7:268.
[10] Demirbas AH, Demirbas I. Importance of rural bioenergy for developing countries. Energy Convers Manag 2007;48:2386–98. https://doi.org/10.1016/J.ENCONMAN.2007.03.005.
[11] Chala GT, Aziz ARA, Hagos FY. Natural gas engine technologies: challenges and energy sustainability issue. Energies 2018;11:2934. https://doi.org/10.3390/EN11112934. 2018;11:2934.
[12] Park G, Mun S, Hong H, Chung T, Jung S, Kim S, et al. Characterization of emission factors concerning gasoline, LPG, and diesel vehicles via transient chassis-dynamometer tests. Appl Sci 2019;9:1573. https://doi.org/10.3390/APP9081573. 2019;9:1573.
[13] Mourad M, Mahmoud K. Investigation into SI engine performance characteristics and emissions fuelled with ethanol/butanol-gasoline blends. Renew Energy 2019;143:762–71. https://doi.org/10.1016/J.RENENE.2019.05.064.
[14] Uslu S, Celik MB. Combustion and emission characteristics of isoamyl alcohol-gasoline blends in spark ignition engine. Fuel 2020;262:116496. https://doi.org/10.1016/J.FUEL.2019.116496.

[15] Shirazi SA, Abdollahipoor B, Windom B, Reardon KF, Foust TD. Effects of blending C3-C4 alcohols on motor gasoline properties and performance of spark ignition engines: a review. Fuel Process Technol 2020;197:106194. https://doi.org/10.1016/J.FUPROC.2019.106194.
[16] Sadiq Al-Baghdadi MAR, Shahad Al-Janabi HAK. Improvement of performance and reduction of pollutant emission of a four stroke spark ignition engine fueled with hydrogen–gasoline fuel mixture. Energy Convers Manag 2000;41:77–91. https://doi.org/10.1016/S0196-8904(99)00080-1.
[17] Awad OI, Mamat R, Ali OM, Sidik NAC, Yusaf T, Kadirgama K, et al. Alcohol and ether as alternative fuels in spark ignition engine: a review. Renew Sustain Energy Rev 2018;82:2586–605. https://doi.org/10.1016/J.RSER.2017.09.074.
[18] Iodice P, Cardone M. Ethanol/gasoline blends as alternative fuel in last generation spark-ignition engines: a review on CO and HC engine out emissions. Energies 2021;14:4034. https://doi.org/10.3390/EN14134034. 2021;14:4034.
[19] Phuangwongtrakul S, Wechsatol W, Sethaput T, Suktang K, Wongwises S. Experimental study on sparking ignition engine performance for optimal mixing ratio of ethanol–gasoline blended fuels. Appl Therm Eng 2016;100:869–79. https://doi.org/10.1016/J.APPLTHERMALENG.2016.02.084.
[20] Al-Hasan M. Effect of ethanol–unleaded gasoline blends on engine performance and exhaust emission. Energy Convers Manag 2003;44:1547–61. https://doi.org/10.1016/S0196-8904(02)00166-8.
[21] Turner D, Xu H, Cracknell RF, Natarajan V, Chen X. Combustion performance of bio-ethanol at various blend ratios in a gasoline direct injection engine. Fuel 2011;90:1999–2006. https://doi.org/10.1016/J.FUEL.2010.12.025.
[22] Elfasakhany A. Investigations on the effects of ethanol–methanol–gasoline blends in a spark-ignition engine: performance and emissions analysis. Eng Sci Technol an Int J 2015;18:713–9. https://doi.org/10.1016/J.JESTCH.2015.05.003.
[23] Sayin C, Balki MK. Effect of compression ratio on the emission, performance and combustion characteristics of a gasoline engine fueled with iso-butanol/gasoline blends. Energy 2015;82:550–5. https://doi.org/10.1016/J.ENERGY.2015.01.064.
[24] Zaharin MSM, Abdullah NR, Masjuki HH, Ali OM, Najafi G, Yusaf T. Evaluation on physicochemical properties of iso-butanol additives in ethanol-gasoline blend on performance and emission characteristics of a spark-ignition engine. Appl Therm Eng 2018;144:960–71. https://doi.org/10.1016/J.APPLTHERMALENG.2018.08.057.
[25] Mohammed MK, Balla HH, Al-Dulaimi ZMH, Kareem ZS, Al-Zuhairy MS. Effect of ethanol-gasoline blends on SI engine performance and emissions. Case Stud Therm Eng 2021;25:100891. https://doi.org/10.1016/J.CSITE.2021.100891.
[26] Anderson JE, Dicicco DM, Ginder JM, Kramer U, Leone TG, Raney-Pablo HE, et al. High octane number ethanol–gasoline blends: quantifying the potential benefits in the United States. Fuel 2012;97:585–94. https://doi.org/10.1016/J.FUEL.2012.03.017.
[27] Qian Y, Liu G, Guo J, Zhang Y, Zhu L, Lu X. Engine performance and octane on demand studies of a dual fuel spark ignition engine with ethanol/gasoline surrogates as fuel. Energy Convers Manag 2019;183:296–306. https://doi.org/10.1016/J.ENCONMAN.2019.01.011.
[28] Starchevskyy V, Ribun V, Kurta S, Khatsevich O. Properties and composition of absolutized ethanol and its effect on the gasoline octane number. Chem Chem Technol 2018;12:346–54. https://doi.org/10.23939/CHCHT12.03.346.
[29] Andersen VF, Anderson JE, Wallington TJ, Mueller SA, Nielsen OJ. Vapor pressures of alcohol-gasoline blends. Energy Fuel 2010;24:3647–54. https://doi.org/10.1021/EF100254W/SUPPL_FILE/EF100254W_SI_001.PDF.
[30] Aghahossein Shirazi S, Abdollahipoor B, Martinson J, Windom B, Foust TD, Reardon KF. Effects of dual-alcohol gasoline blends on physiochemical properties and volatility behavior. Fuel 2019;252:542–52. https://doi.org/10.1016/J.FUEL.2019.04.105.
[31] Hua Y, Qiu L, Liu F, Qian Y, Meng S. Numerical investigation into the effects of oxygen concentration on flame characteristics and soot formation in diffusion and partially premixed flames. Fuel 2020;268:117398. https://doi.org/10.1016/J.FUEL.2020.117398.
[32] Chen M, Liu D, Jiang B. Soot formation and combustion characteristics in confined mesoscale combustors under conventional and oxy-combustion conditions (O2/N2 and O2/CO2). Fuel 2020;264:116808. https://doi.org/10.1016/J.FUEL.2019.116808.
[33] Koivisto E, Ladommatos N, Gold M. Systematic study of the effect of the hydroxyl functional group in alcohol molecules on compression ignition and exhaust gas emissions. Fuel 2015;153:650–63. https://doi.org/10.1016/J.FUEL.2015.03.042.
[34] Sahu TK, Shukla PC. Effect of inherent oxygen mass fraction of alcohol blends with diesel on combustion and emission parameters. Environ Prog Sustain Energy 2023;42:e14030. https://doi.org/10.1002/EP.14030.
[35] Edwin Geo V, Jesu Godwin D, Thiyagarajan S, Saravanan CG, Aloui F. Effect of higher and lower order alcohol blending with gasoline on performance, emission and combustion characteristics of SI engine. Fuel 2019;256:115806. https://doi.org/10.1016/J.FUEL.2019.115806.
[36] Emiroğlu AO, Şen M. Combustion, performance and emission characteristics of various alcohol blends in a single cylinder diesel engine. Fuel 2018;212:34–40. https://doi.org/10.1016/J.FUEL.2017.10.016.
[37] Balki MK, Sayin C, Canakci M. The effect of different alcohol fuels on the performance, emission and combustion characteristics of a gasoline engine. Fuel 2014;115:901–6. https://doi.org/10.1016/J.FUEL.2012.09.020.
[38] Simsek S, Uslu S, Simsek H. Evaluation of the effect of a new alternative fuel containing boron and hydrogen on gasoline engine performance and emission responses. Int J Environ Sci Technol 2022;19:4913–22. https://doi.org/10.1007/S13762-021-03460-6/FIGURES/10.
[39] Lee JG, Weismiller M, Connell TL, Risha GA, Yetter RA, Gilbert PD, et al. Ammonia borane based-propellants. 44th AIAA/ASME/SAE/ASEE Jt Propuls Conf Exhib 2008. https://doi.org/10.2514/6.2008-5037.
[40] Gültekin E, Calam A, Şahin M. Experimental investigation of trimethyl borate as a fuel additive for a SI engine. Energy Sources, Part A Recover Util Environ Eff 2023;45:419–33. https://doi.org/10.1080/15567036.2023.2171516.
[41] Pfeil MA, Groven LJ, Lucht RP, Son SF. Effects of ammonia borane on the combustion of an ethanol droplet at atmospheric pressure. Combust Flame 2013;160:2194–203. https://doi.org/10.1016/J.COMBUSTFLAME.2013.04.014.
[42] Simsek S, Uslu S, Simsek H. Evaluation of the effect of a new alternative fuel containing boron and hydrogen on gasoline engine performance and emission responses. Int J Environ Sci Technol 2022;19:4913–22. https://doi.org/10.1007/S13762-021-03460-6/FIGURES/10.
[43] Veeraraghavan Ramachandran P, Kulkarni AS, Pfeil MA, Dennis JD, Willits JD, Heister SD, et al. Amine–boranes: green hypergolic fuels with consistently low ıgnition delays. Chem Eur J 2014;20:16869–72. https://doi.org/10.1002/CHEM.201405224.
[44] Pfeil MA, Kulkarni AS, Ramachandran PV, Son SF, Heister SD. Solid amine–boranes as high-performance and hypergolic hybrid rocket fuels, vol. 32; 2015. p. 23–31. https://doi.org/10.2514/1.B35591. Https://DoiOrg/102514/1B35591.
[45] Bowden ME, Brown IWM, Gainsford GJ, Wong H. Structure and thermal decomposition of methylamine borane. Inorganica Chim Acta 2008;361:2147–53. https://doi.org/10.1016/J.ICA.2007.10.034.
[46] Szilágyi P, Hunter S, Morrison CA, Tang CC, Pulham CR. Pressure-induced structural changes in methylamine borane and dimethylamine borane. J Alloys Compd 2017;722:953–61. https://doi.org/10.1016/J.JALLCOM.2017.06.174.
[47] Aldridge S, Downs AJ, Tang CY, Parsons S, Clarke MC, Johnstone RDL, et al. Structures and aggregation of the methylamine-borane molecules, $Me_nH_{3-n}N{\bullet}BH_3$ (n = 1-3), studied by X-ray diffraction, gas-phase electron diffraction, and quantum chemical calculations. J Am Chem Soc 2009;131:2231–43. https://doi.org/10.1021/JA807545P/SUPPL_FILE/JA807545P_SI_004.PDF.
[48] Pal S, Kusumoto S, Nozaki K. Dehydrogenation of dimethylamine-borane catalyzed by half-sandwich ır and rh complexes: mechanism and the role of Cp* noninnocence. Organometallics 2018;37:906–14. https://doi.org/10.1021/ACS.ORGANOMET.7B00889.
[49] Huo J, Zhang K, Wei H, Fu L, Zhao C, He C, et al. A review on hydrogen production from ammonia borane: experimental and theoretical studies. Chinese Chem Lett 2023;34:108280. https://doi.org/10.1016/J.CCLET.2023.108280.
[50] Demirci UB. Ammonia borane, a material with exceptional properties for chemical hydrogen storage. Int J Hydrogen Energy 2017;42:9978–10013. https://doi.org/10.1016/J.IJHYDENE.2017.01.154.
[51] Karataş Y, Çetin T, Akkuş IN, Akinay Y, Gülcan M. Rh (0) nanoparticles impregnated on two-dimensional transition metal carbides, MXene, as an effective nanocatalyst for ammonia-borane hydrolysis. Int J Energy Res 2022;46:11411–23. https://doi.org/10.1002/ER.7938.
[52] Karataş Y, Zengin A, Gülcan M. Preparation and characterization of amine-terminated delafossite type oxide, $CuMnO_2$–NH_2, supported Pd (0) nanoparticles for the H_2 generation from the methanolysis of ammonia-borane. Int J Hydrogen Energy 2022;47:16036–46. https://doi.org/10.1016/J.IJHYDENE.2022.03.098.
[53] Karataş Y, Gülcan M, Çelebi M, Zahmakiran M. Pd(0) nanoparticles decorated on graphene nanosheets (gns): synthesis, definition and testing of the catalytic performance in the methanolysis of ammonia borane at room conditions. ChemistrySelect 2017;2:9628–35. https://doi.org/10.1002/SLCT.201701616.
[54] Ramachandran PV, Gagare PD. Preparation of ammonia borane in high yield and purity, methanolysis, and regeneration. Inorg Chem 2007;46:7810–7. https://doi.org/10.1021/IC700772A/SUPPL_FILE/IC700772A-FILE003.CIF.
[55] Kantürk Figen A, Pişkin MB, Coşkuner B, Imamoğlu V. Synthesis, structural characterization, and hydrolysis of ammonia borane (NH_3BH_3) as a hydrogen storage carrier. Int J Hydrogen Energy 2013;38:16215–28. https://doi.org/10.1016/J.IJHYDENE.2013.10.033.
[56] Holman JP. Experimental methods for engineers, vols. McGrawHill Book Company; 1971. p. 37–52.
[57] Stephens FH, Pons V, Baker RT. Ammonia–borane: the hydrogen source par excellence? Dalt Trans 2007:2613–26. https://doi.org/10.1039/B703053C.
[58] Hannauer J, Demirci UB, Geantet C, Herrmann JM, Miele P. Enhanced hydrogen release by catalyzed hydrolysis of sodium borohydride–ammonia borane mixtures: a solution-state ^{11}B-NMR study. Phys Chem Chem Phys 2011;13:3809–18. https://doi.org/10.1039/C0CP02090G.
[59] Kang X, Ma L, Fang Z, Gao L, Luo J, Wang S, et al. Promoted hydrogen release from ammonia borane by mechanically milling with magnesium hydride: a new destabilizing approach. Phys Chem Chem Phys 2009;11:2507–13. https://doi.org/10.1039/B820401B.
[60] Ramachandran PV, Kulkarni AS. The role of ammonia in promoting ammonia borane synthesis. Dalton Trans 2016;45:16433–40. https://doi.org/10.1039/C6DT02925F.
[61] Arulsamy N. Ammonia borane acid−base complex: an experiment ınvolving ^{1}H and ^{11}B NMR spectroscopy and the gas laws. J Chem Educ 2018;95:1381–5. https://doi.org/10.1021/acs.jchemed.8b00038.
[62] Singh AK, Mishra VP, Barman S, Tiwari K, Mondal P, Barman N. Study of emission characteristics and performance analysis of ethanol diesel blend. NanoWorld J 2023;9:S369–73. https://doi.org/10.17756/NWJ.2023-S1-072.
[63] Sharudin H, Abdullah NR, Najafi G, Mamat R, Masjuki HH. Investigation of the effects of iso-butanol additives on spark ignition engine fuelled with methanol-gasoline blends. Appl Therm Eng 2017;114:593–600. https://doi.org/10.1016/J.APPLTHERMALENG.2016.12.017.

[64] Feng H, Zhang H, Wei J, Li B, Wang D. The influence of mixing ratio of low carbon mixed alcohols on knock combustion of spark ignition engines. Fuel 2019;240:339–48. https://doi.org/10.1016/J.FUEL.2018.12.005.
[65] Altun S, Oztop HF, Oner C, Varol Y. Exhaust emissions of methanol and ethanol-unleaded gasoline blends in a spark ignition engine. Therm Sci 2013;17:291–7. https://doi.org/10.2298/TSCI111207034A.
[66] Elfasakhany A. Performance and emissions analysis on using acetone–gasoline fuel blends in spark-ignition engine. Eng Sci Technol an Int J 2016;19:1224–32. https://doi.org/10.1016/J.JESTCH.2016.02.002.
[67] Yakın A, Cabir B. Effects of adding phthalocyanine to gasoline fuel on engine performance and exhaust emissions ın spark ıgnition engine. Heat Tran Res 2024;55(14):33–46. https://doi.org/10.1615/HeatTransRes.2024052012.
[68] Cabir B, Yakın A. Evaluation of gasoline-phthalocyanines fuel blends in terms of engine performance and emissions in gasoline engines. J Energy Inst 2024;112:101483. https://doi.org/10.1016/j.joei.2023.101483.
[69] Momani W. The effects of excess oxygen to mixture on the gasses emissions of a gasoline engine. Am J Appl Sci 2009;6:1122–5. https://doi.org/10.3844/AJASSP.2009.1122.1125.
[70] Lemaire R, Boudreau A, Seers P. Performance and emissions of a DISI engine fueled with gasoline/ethanol and gasoline/C-4 oxygenate blends – development of a PM index correlation for particulate matter emission assessment. Fuel 2019;241:1172–83. https://doi.org/10.1016/J.FUEL.2018.12.007.
[71] Lim CS, Lim JH, Cha JS, Lim JY. Comparative effects of oxygenates-gasoline blended fuels on the exhaust emissions in gasoline-powered vehicles. J Environ Manage 2019;239:103–13. https://doi.org/10.1016/J.JENVMAN.2019.03.039.
[72] Gilazhov YG, Kulbatyrov DK, Togaybayeva AG, Zholdaskalieva AZ. Effectiveness of methyl tert-butyl ether and ethynylcyclohexanol on increasing the octane number of gasoline compositions of straightrun gasoline + reforming. Bull Shakarim Univ Tech Sci 2023;0:73–81. https://doi.org/10.53360/2788-7995-2023-3(11)-9.
[73] Nguyen DD, Moghaddam H, Pirouzfar V, Fayyazbakhsh A, Su CH. Improving the gasoline properties by blending butanol-Al_2O_3 to optimize the engine performance and reduce air pollution. Energy 2021;218:119442. https://doi.org/10.1016/J.ENERGY.2020.119442.
[74] Manzetti S, Andersen O. A review of emission products from bioethanol and its blends with gasoline. Background for new guidelines for emission control. Fuel 2015;140:293–301. https://doi.org/10.1016/J.FUEL.2014.09.101.
[75] Wen L bin, Xin CY, Yang SC. The effect of adding dimethyl carbonate (DMC) and ethanol to unleaded gasoline on exhaust emission. Appl Energy 2010;87:115–21. https://doi.org/10.1016/J.APENERGY.2009.06.005.
[76] Schirmer WN, Olanyk LZ, Guedes CLB, Quessada TP, Ribeiro CB, Capanema MA. Effects of air/fuel ratio on gas emissions in a small spark-ignited non-road engine operating with different gasoline/ethanol blends. Environ Sci Pollut Res 2017;24:20354–9. https://doi.org/10.1007/s11356-017-9651-8.
[77] Tibaquirá JE, Huertas JI, Ospina S, Quirama LF, Niño JE. The effect of using ethanol-gasoline blends on the mechanical, energy and environmental performance of ın-use vehicles. Energies 2018;11:221. https://doi.org/10.3390/EN11010221.
[78] Tsai JH, Ko YL, Huang CM, Chiang HL. Effects of blending ethanol with gasoline on the performance of motorcycle catalysts and airborne pollutant emissions. Aerosol Air Qual Res 2019;19:2781–92. https://doi.org/10.4209/AAQR.2019.10.0539.
[79] Yakın A, Behçet R. Effect of different types of fuels tested in a gasoline engine on engine performance and emissions. Int J Hydrogen Energy 2021;46:33325–38. https://doi.org/10.1016/J.IJHYDENE.2021.07.133.
[80] Gu X, Huang Z, Cai J, Gong J, Wu X, Lee CF. Emission characteristics of a spark-ignition engine fuelled with gasoline-n-butanol blends in combination with EGR. Fuel 2012;93:611–7. https://doi.org/10.1016/J.FUEL.2011.11.040.
[81] Iodice P, Senatore A, Langella G, Amoresano A. Effect of ethanol-gasoline blends on CO and HC emissions in last generation SI engines within the cold-start transient: an experimental investigation. Appl Energy 2016;179:182–90. https://doi.org/10.1016/J.APENERGY.2016.06.144.
[82] Jhang SR, Lin YC, Chen KS, Lin SL, Batterman S. Evaluation of fuel consumption, pollutant emissions and well-to-wheel GHGs assessment from a vehicle operation fueled with bioethanol, gasoline and hydrogen. Energy 2020;209:118436. https://doi.org/10.1016/J.ENERGY.2020.118436.
[83] Wang X, Chen Z, Ni J, Liu S, Zhou H. The effects of hydrous ethanol gasoline on combustion and emission characteristics of a port injection gasoline engine. Case Stud Therm Eng 2015;6:147–54. https://doi.org/10.1016/J.CSITE.2015.09.007.
[84] Al-Harbi AA, Alabduly AJ, Alkhedhair AM, Alqahtani NB, Albishi MS. Effect of operation under lean conditions on NO_x emissions and fuel consumption fueling an SI engine with hydrous ethanol–gasoline blends enhanced with synthesis gas. Energy 2022;238:121694. https://doi.org/10.1016/J.ENERGY.2021.121694.
[85] Mirhashemi FS, Sadrnia H. NO_x emissions of compression ignition engines fueled with various biodiesel blends: a review. J Energy Inst 2020;93:129–51. https://doi.org/10.1016/J.JOEI.2019.04.003.
[86] Jin B, Wang M, Zhu R, Jia M, Wang Y, Li S, et al. Evaluation of additives used in gasoline vehicles in China: fuel economy, regulated gaseous pollutants and volatile organic compounds based on both chassis dynamometer and on-road tests. Clean Technol Environ Policy 2021;23:1967–79. https://doi.org/10.1007/S10098-021-02090-3.
[87] Nie X, Bi Y, Shen L, Lei J, Wan M, Wang Z, Huang F. Combustion and emission characteristics of ammonia-diesel dual fuel engine at different altitudes. Fuel 2024;371:132072. https://doi.org/10.1016/j.fuel.2024.132072.
[88] Liu S, Lin Z, Qi Y, Wang Z, Yang D, Lu G, Wang B. Combustion and emission characteristics of a spark ignition engine fueled with ammonia/gasoline and pure ammonia. Appl Energy 2024;369:123538. https://doi.org/10.1016/j.apenergy.2024.123538.
[89] Göksu TT. Enhancing cooling efficiency: innovative geometric designs and mono-hybrid nanofluid applications in heat sinks. Case Stud Therm Eng 2024:104096.
[90] Göksu TT. Investigation of pin and perforated heatsink cooling efficiency and temperature distribution. Journal of Thermal Analysis and Calorimetry 2024:1–13.